



HAL
open science

Disentangling internal and external contributions to Atlantic multidecadal variability over the past millennium

Shih-Wei Fang, Myriam Khodri, Claudia Timmreck, Davide Zanchettin,
Johann Jungclaus

► **To cite this version:**

Shih-Wei Fang, Myriam Khodri, Claudia Timmreck, Davide Zanchettin, Johann Jungclaus. Disentangling internal and external contributions to Atlantic multidecadal variability over the past millennium. *Geophysical Research Letters*, 2021, 48 (23), 10.1029/2021gl095990 . hal-03530833

HAL Id: hal-03530833

<https://hal.science/hal-03530833>

Submitted on 18 Jan 2022

HAL is a multi-disciplinary open access archive for the deposit and dissemination of scientific research documents, whether they are published or not. The documents may come from teaching and research institutions in France or abroad, or from public or private research centers.

L'archive ouverte pluridisciplinaire **HAL**, est destinée au dépôt et à la diffusion de documents scientifiques de niveau recherche, publiés ou non, émanant des établissements d'enseignement et de recherche français ou étrangers, des laboratoires publics ou privés.



Distributed under a Creative Commons Attribution 4.0 International License

Geophysical Research Letters[®]



RESEARCH LETTER

10.1029/2021GL095990

Key Points:

- The internal and external contributions to Atlantic multidecadal variability (AMV) over the past millennium can be separated by a pattern-based calculation of AMV
- The internal AMV has a robust tripole pattern and dominates the relationship with meridional overturning circulation
- The North Atlantic response to post-eruption global cooling has a damped behavior and is identified as a more uniform spatial pattern

Supporting Information:

Supporting Information may be found in the online version of this article.

Correspondence to:

S.-W. Fang,
shih-wei.fang@mpimet.mpg.de

Citation:

Fang, S.-W., Khodri, M., Timmreck, C., Zanchettin, D., & Jungclauss, J. (2021). Disentangling internal and external contributions to Atlantic multidecadal variability over the past millennium. *Geophysical Research Letters*, 48, e2021GL095990. <https://doi.org/10.1029/2021GL095990>

Received 7 SEP 2021

Accepted 8 NOV 2021





Author Contributions:

Conceptualization: Shih-Wei Fang, Myriam Khodri, Claudia Timmreck, Davide Zanchettin, Johann Jungclauss
Data curation: Shih-Wei Fang, Myriam Khodri, Claudia Timmreck, Johann Jungclauss
Formal analysis: Shih-Wei Fang
Funding acquisition: Myriam Khodri, Claudia Timmreck
Investigation: Shih-Wei Fang, Myriam Khodri, Claudia Timmreck, Davide Zanchettin, Johann Jungclauss
Methodology: Shih-Wei Fang

© 2021. The Authors.

This is an open access article under the terms of the [Creative Commons Attribution License](https://creativecommons.org/licenses/by/4.0/), which permits use, distribution and reproduction in any medium, provided the original work is properly cited.

Disentangling Internal and External Contributions to Atlantic Multidecadal Variability Over the Past Millennium

Shih-Wei Fang¹ , Myriam Khodri², Claudia Timmreck¹ , Davide Zanchettin³ , and Johann Jungclauss¹ 

¹Max-Planck-Institut für Meteorologie, Hamburg, Germany, ²IRD/IPSL/Laboratoire d'Océanographie et du Climat, Paris, France, ³University Ca' Foscari of Venice, Venice, Italy

Abstract The Atlantic multidecadal variability (AMV) modulates the North Atlantic surface ocean variability and affects decadal climates over the globe; its underlying mechanisms remain, however, under debate. In this study, we use a multi-model ensemble of transient past-millennium (850–1849) and unperturbed preindustrial control simulations contributing to the paleoclimate modeling intercomparison project—phase 4 (PMIP4) to decompose the AMV signal into the internal AMV and the external signal. The internal component of AMV exhibits no robust behavior across simulations during periods of major forcing such as strong volcanic eruptions, whereas the external forced temperature responds to volcanic eruptions with an immediate radiative cooling followed, in some simulations, by a sequence of damped multidecadal oscillations. The internal component tightly relates with the Atlantic meridional overturning circulation (AMOC) and dominates the fluctuations of AMV; whereas the external signal has limited impacts on AMOC and explains ~25% of the AMV variance over the past millennium.

Plain Language Summary The decadal-scale changes of the sea surface temperature over the North Atlantic is referred to as the Atlantic multidecadal variability (AMV), which modulates the North Atlantic surface ocean variability and affects decadal climates over the globe; however, how different forcing processes can affect AMV remains debated. In this study, a multi-model ensemble participating in the paleoclimate modeling intercomparison project—phase 4 (PMIP4) of preindustrial millennium simulation (850–1849 CE) is used to decompose the AMV signal into the internal AMV and the external signal and to compare it with the preindustrial control simulation not including external forcing (such as volcanic eruptions, solar irradiance, and anthropogenic greenhouse gas). The internal component of AMV exhibits no robust signature across simulations during periods of major forcing such as strong volcanic eruptions, whereas the external forced temperature responds to volcanic eruptions with an immediate radiative cooling followed, in some simulations, by a sequence of damped multidecadal oscillations. The internal component of AMV tightly relates with the Atlantic subsurface ocean circulation called Atlantic meridional overturning circulation (AMOC) and dominates the variations of AMV, while the external signal has limited impacts on AMOC and explains ~25% of the AMV variance over past millennium.

1. Introduction

The Atlantic multidecadal variability (AMV) is a basinwide fluctuation on 50–80-year timescales in the surface ocean state of the North Atlantic, generally defined by a characteristic horseshoe shape in North Atlantic sea-surface temperature (SST) anomalies (Enfield et al., 2001; Goldenberg et al., 2001). This multidecadal variability has been studied intensively over the past few decades due to its observed control on decadal climates for regions around the Atlantic Ocean, such as Sahel (Knight et al., 2006; Martin et al., 2014; Villamayor et al., 2018; Zhang & Delworth, 2006), North America (Enfield et al., 2001; Ruprich-Robert et al., 2018), and Eurasia (O'Reilly et al., 2017; Sutton & Dong, 2012; Sutton & Hodson, 2005), as well as for remote regions and climate phenomena, such as El Niño-Southern Oscillation/Equatorial Pacific (Dong et al., 2006; Ruprich-Robert et al., 2021; Yu et al., 2015; Zanchettin, Bothe, Graf, et al., 2016), Pacific subtropical mode water (Wu et al., 2020), and Antarctic sea-ice extent (Li et al., 2014). Even though its climate impacts are well-documented, the physical mechanisms and underlying processes causing AMV are not completely understood.

Project Administration: Claudia Timmreck, Johann Jungclauss
Resources: Shih-Wei Fang, Myriam Khodri, Claudia Timmreck, Johann Jungclauss
Software: Shih-Wei Fang
Supervision: Myriam Khodri, Claudia Timmreck, Davide Zanchettin, Johann Jungclauss
Validation: Shih-Wei Fang
Visualization: Shih-Wei Fang
Writing – original draft: Shih-Wei Fang
Writing – review & editing: Shih-Wei Fang, Myriam Khodri, Claudia Timmreck, Davide Zanchettin, Johann Jungclauss

One difficulty in studying the AMV dynamics is the lack of robustness across index definitions, which has brought further uncertainties regarding characteristic timescale and spatial pattern associated with the AMV (Zanchettin et al., 2014; Zhang et al., 2019). The AMV obtained by linearly detrended SST anomalies can only capture the horseshoe warming (Otterå et al., 2010) without a tripole structure. In contrast, when applying more elaborate statistical approaches (Czaja & Frankignoul, 2002; Wallace et al., 1990), the horseshoe structure of SST anomalies exists as a tripole structure with cooling located around 20–40°N and warmings at above 40°N and below 20°N. The short window of observations and lack of consistency among climate models regarding the AMV structure and frequency further complicates the understanding of underlying dynamics, either related to internal processes to the climate system or SST fingerprints from external forcing factors (Mann et al., 2021; Zanchettin, Bothe, Rubino, & Jungclauss, 2016).

The internal component of AMV, which is not driven by external forcing (e.g., volcanic eruption, solar irradiance, or anthropogenic aerosol), is often related to large-scale stochastic atmospheric forcing such as surface heat, momentum, and freshwater fluxes associated with the North Atlantic oscillation (NAO) (Clement et al., 2015). The Atlantic meridional ocean circulation (AMOC) can also modulate North Atlantic SST through ocean heat transport convergence (Oelsmann et al., 2020; Zhang et al., 2019). Multi-model analysis of unperturbed simulations demonstrates that both large-scale atmospheric variability and oceanic processes imprint on AMV with variable strength in the course of multi-centennial periods (Zanchettin, Bothe, Rubino, & Jungclauss, 2016).

On the other hand, an externally forced component of the AMV can be driven by changes in anthropogenic aerosol, solar variations, and large volcanic eruptions (Booth et al., 2012; Otterå et al., 2010; Zanchettin et al., 2013). The external forcing can imprint on North Atlantic SST not only by directly heating or cooling the surface ocean, but also by changing the atmospheric and oceanic circulation. These intertwined processes further complicate the identification of the key sources generating the AMV and the relative importance between the internally and externally generated AMV. Wang et al. (2017) suggests the externally forced variations of AMV are responsible for 30% of total AMV, thereby emphasizing the importance of internal processes (Zhang et al., 2019). In contrast, Mann et al. (2021) argues the AMV is mainly a result from external forcing due to its characteristic timescale aligned with the pacing of strong volcanic eruptions and the lack of robust AMV timescale in the multi-model ensemble of unperturbed simulations.

Recent studies have tried to decompose the internally and externally driven AMV from the traditional AMV index. For example, Qin et al. (2020a) and others (O'Reilly et al., 2019; Wang et al., 2017) calculate the internal AMV index by removing the estimate of externally forced components from the traditional AMV index and make use of temporal relations between forced and unperturbed simulations. In this study, we apply, in contrast, a spatial pattern-based criterion that extracts the relative importance of the internal AMV and the external forced signature and introduces a unique perspective in understanding how natural external forcing impacts the AMV over the pre-industrial millennium (850–1849 CE) when anthropogenic forcing is weak.

2. Datasets and Methods

Monthly mean values of variables including SST, sea-level pressure and meridional overturning streamfunction, are obtained for the piControl and past1000 (850–1849 CE) simulations from four state-of-the-art models participating in the fourth phase of the paleoclimate modeling intercomparison project (PMIP4; Jungclauss et al., 2017; Kageyama et al., 2018). The MPI-ESM1-2-LR (Mauritsen et al., 2019) was run by the Max Planck Institute for Meteorology (MPI-M); MIROC-ES2L (Ohgaito et al., 2021) by the Japan Agency for Marine-Earth Science and Technology (JAMSTEC), Atmosphere and Ocean Research Institute (AORI), National Institute for Environmental Studies (NIES), and RIKEN Center for Computational Science (R-CCS) (MIROC), MRI-ESM2-0 by the Meteorological Research Institute (MRI; Yukimoto, Kawai, et al., 2019), and IPSL-CM6A-LR by the Institut Pierre Simon Laplace (IPSL; Boucher et al., 2020; Lurton et al., 2020). A short model overview is given in Table S1. Anomalies are calculated by removing the mean annual cycle over the entire period and are high-pass filtered with a frequency cutoff at 100-years in order to remove any very long-term trend instead of removing a linear trend.

We use the term, “typical-AMV” index, to stand for the AMV index following the conventional definition (Enfield et al., 2001; Zhang et al., 2016), which averages SST anomalies spatially over the North Atlantic (0°N–60°N, 80°W–0°W) with a 10-year running mean. For each model, the spatial regression pattern associated with the typical-AMV index in piControl is considered as representative of the internal AMV pattern (Figures 1a–1d).

Regression of AMVs onto SST anomalies

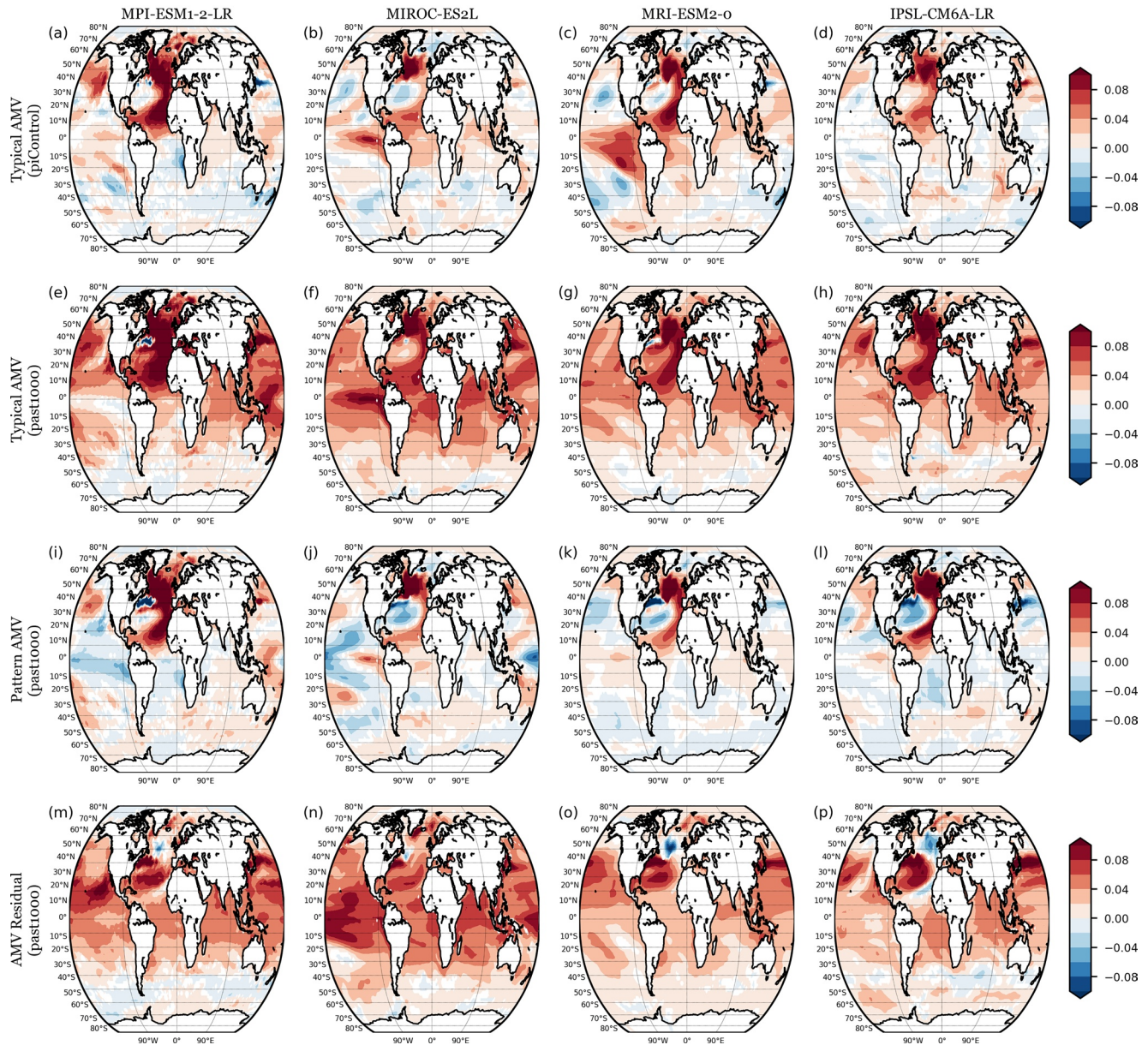


Figure 1. (a)–(d) Regression of typical-AMV onto SST anomalies in piControl, (e)–(h) typical-AMV in past1000, (i)–(l) pattern-AMV index in past1000, and (m)–(p) AMV-residual index in past1000.

Projection of this spatial pattern onto the 10-year lowpass filtered SST anomalies of both piControl and past1000 simulations yields an index that we refer to as pattern-AMV index (Figures 1i–1l). The pattern-AMV index differs from the typical-AMV index as the former describes variations in the amplitude and sign of the stationary internal AMV pattern, whereas the latter describes variations of basin-average SST independent of any spatial pattern. The index difference between typical- and pattern-AMV index is defined as AMV-residual index (Figures 1m–1p), which represents the North Atlantic SST variability that is not related to the internal AMV instantaneously. As there are unlimited spatial distributions besides the internal AMV structure, the AMV-residual index can also be viewed as a North Atlantic warming/cooling captured by an uniform temperature change (Figures S1 and S2). Further details on the method are provided in the supplementary material (Text S1 in Supporting Information S1; Chiang & Vimont, 2004).

The AMOC index is defined as the maximum meridional overturning streamfunction zonally integrated across the Atlantic basin at 30°N latitude and below 1,000 m depth.

The occurrence of strong tropical volcanic eruptions is identified based on tropical mean outgoing shortwave radiation flux at the top of the atmosphere. Specifically, the month of an event corresponds to the first month when the anomaly of all models exceeds 5 W/m². In order to avoid the impact from previous eruptions, the event is discarded if it occurs earlier than 20 years after the previous identified event (Table S2).

3. Results

Figures 1i–1p show the SST regressions of the pattern- and AMV-residual index over the past millennium. Similar to the SST structure of the typical-AMV in piControl (Figures 1a–1d), the pattern-AMVs in past1000 (Figures 1i–1l) have a shape expressing a tripole structure in the northern Atlantic with negative SSTs sitting around 30°N. The warming signature appears most pronounced in the subpolar region, which is consistent with the strong control of AMV found there in observations (Friedman et al., 2017). Though showing the tripole structure, the SST distributions are distinct in details among models, but we diagnose that each model exhibits similar structures between the piControl and past1000 simulations. In contrast, ocean-basins other than the North Atlantic show no agreement between models and have generally weaker signals. The similar structure as the typical-AMV in piControl, as expected, confirms the representation of the internal component of AMV in past1000 for the pattern-AMV index.

On the other hand, the SST patterns of the AMV-residual exhibit a warming spreading over the northern hemisphere, including positive anomalies in the North Pacific, North Atlantic, and Arctic Oceans. The warming also occurs in the southern hemisphere, although the magnitude is smaller, and the consistency is weaker between models. The IPSL-CM6A-LR has a more similar structure as for the internal-AMV compared to other models. The global SST signature indicates that the AMV-residual index in the past1000 experiments is related more to global climate changes than to basin-scale dynamics. In piControl, the AMV-residual has an opposite phase of the SST structure in the North Atlantic compared to its pattern- and typical-AMV, and does not have a northern hemisphere warming as in past1000 (comparing Figure S3 and Figures 1m–1p). The contrast between the AMV-residual patterns in past1000 and piControl (reflecting mostly global changes and basin-scale dynamics in the North Atlantic, respectively) highlights how this component of AMV involves a variety of processes, and is therefore difficult to be interpreted physically. The extensive signature of the AMV-residual across all basins in the World Ocean suggests this component of North Atlantic SST variability pertains to a Global Multidecadal Variability mode, which requires further studies to be established.

Figure 2a shows the temporal evolution of the pattern-AMV index over the past millennium. The pattern-AMV index exhibits multidecadal fluctuations in all models, whose amplitude and phase disagree across the model ensemble. This lack of robust amplitude and phase at any given time means that the mechanism(s) associated with the pattern-AMV have limited susceptibility from the external forcing and continue operating in transient conditions. After strong tropical volcanic eruptions (Figure S4), the typical-AMV index has strong negative response right after the volcanic eruptions, but the pattern-AMV index shows no significant response in all models, each having a distinct tendency (Figures S4e–S4h). For instance, MPI-ESM1-2-LR yields a weak negative signature 7–10 years after major tropical eruptions, while MRI-ESM2-0 has a weak positive signature after 10 years.

To understand the mechanisms related to the pattern-AMV, we further regress the pattern-AMV index onto the sea-level pressure and meridional overturning streamfunction anomalies (Figures 2b–2h), and surface heat flux (not shown). The pattern-AMV has a very similar signature in the sea-level pressure over models, where positive anomalies exist in the Arctic polar region and negative anomalies appear in the subpolar region, especially over the Atlantic Ocean. This result is consistent with the strong relations between the positive AMV and the negative phase of the Arctic oscillation/North Atlantic oscillation (AO/NAO). The consensus of the signature across models indicates the importance of the atmospheric response in interacting with the pattern-AMV. On the other hand, consensus lacks across models about the pattern-AMV signature on the meridional overturning streamfunction, where MPI-ESM1-2-LR shows a generally enhanced upper branch of the AMOC; MRI-ESM2-0 has opposite values between its tropical and subtropical branch, and IPSL-CM6A-LR indicates much smaller changes. Similar results can also be found in the instantaneous and lagged regression onto surface heat flux, where limited agreement is found across the models. That is, each simulation in past1000 has its own processes and relative

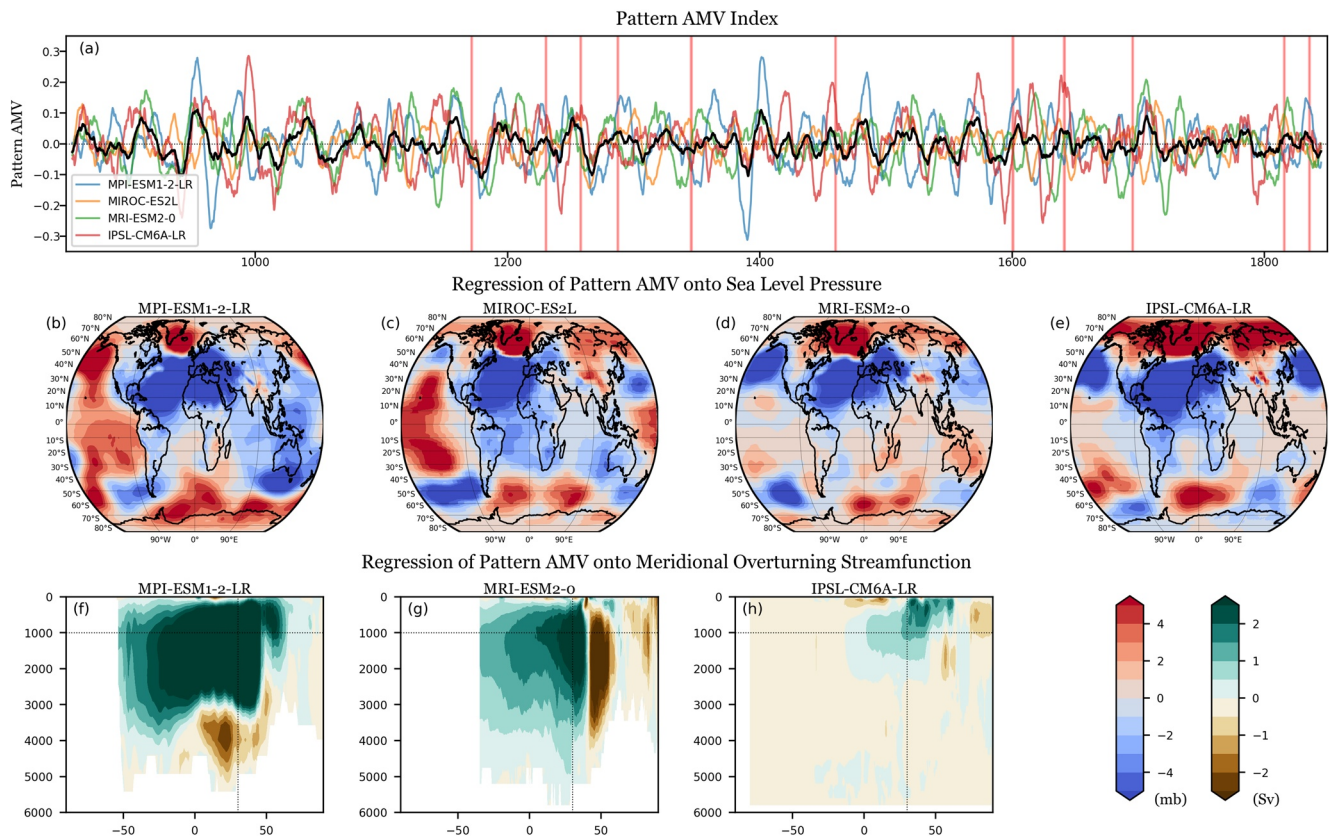


Figure 2. (a) Pattern-AMV index of past1000. Color lines indicate individual models, the black line shows the model mean. Vertical lines indicate large volcanic eruptions. (b)–(e) Regression of the pattern-AMV onto 10-year low-passed sea-level pressure anomalies (mb) in past1000, (f)–(h) for meridional overturning streamfunction anomalies (Sverdrup) in the Atlantic Ocean with y-axis for depth (m) and x-axis for latitude (°N). The strength of the regression values is corresponding to one standard deviation of the patten-AMV index.

importance between the surface and deep ocean in generating the internal variability of AMV, which is also observed consistently in the piControl simulations.

Figure 3a shows the AMV-residual index for the past millennium. Unlike the pattern-AMV, the AMV-residual index exhibits coherent variations across models during specific periods and significant responses to strong tropical volcanic eruptions (Figure 3a). It displays strong negative anomalies immediately after the eruptions as seen in the typical-AMV and bounces back after around 5 years (Fig. S4). As the AMV-residual is tightly related to global temperature changes, this immediate cooling can be interpreted as radiative responses to volcanic forcing, where almost the entire northern hemisphere undergoes a cooling (Figures 1m–1p). Interestingly, after five years in a cold state the AMV-residual index tends to not only bounce back to neutral but, in some models, even bump toward positive values, indicating a possibility of an oscillatory mechanism in the North Atlantic triggered by strong tropical volcanic eruptions (Figures S4i–S4l).

Figures 3b–3e show the sea-level pressure regression of the AMV-residual, where low-pressure anomalies are located in the polar region and high-pressure anomalies in the subtropical region. It is opposite to the structure for the pattern-AMV, but not leading to a tripole structure in the SST, indicating a distinct coupling between the surface ocean and the surface atmosphere in both AMV components. This distribution may be linked to the SST response to volcanic radiative forcing, which reduces the incoming solar radiation at the surface leading to surface cooling especially in the tropical and subtropical regions. Therefore, the AMV, whose total variability is expressed by the typical-AMV, does include a (volcanically) forced component, captured by the AMV-residual, which can be separated by the internal component, captured by the pattern-AMV. Previous studies have found that removing global mean SST signature can better capture the AMV representing only the North Atlantic basin (Yan et al., 2019). By doing so, our pattern-AMV index in past1000 changes only negligibly, while the AMV-residual index is no longer dominated by instantaneous volcanic responses but by delayed dynamical responses with a warming SST pattern

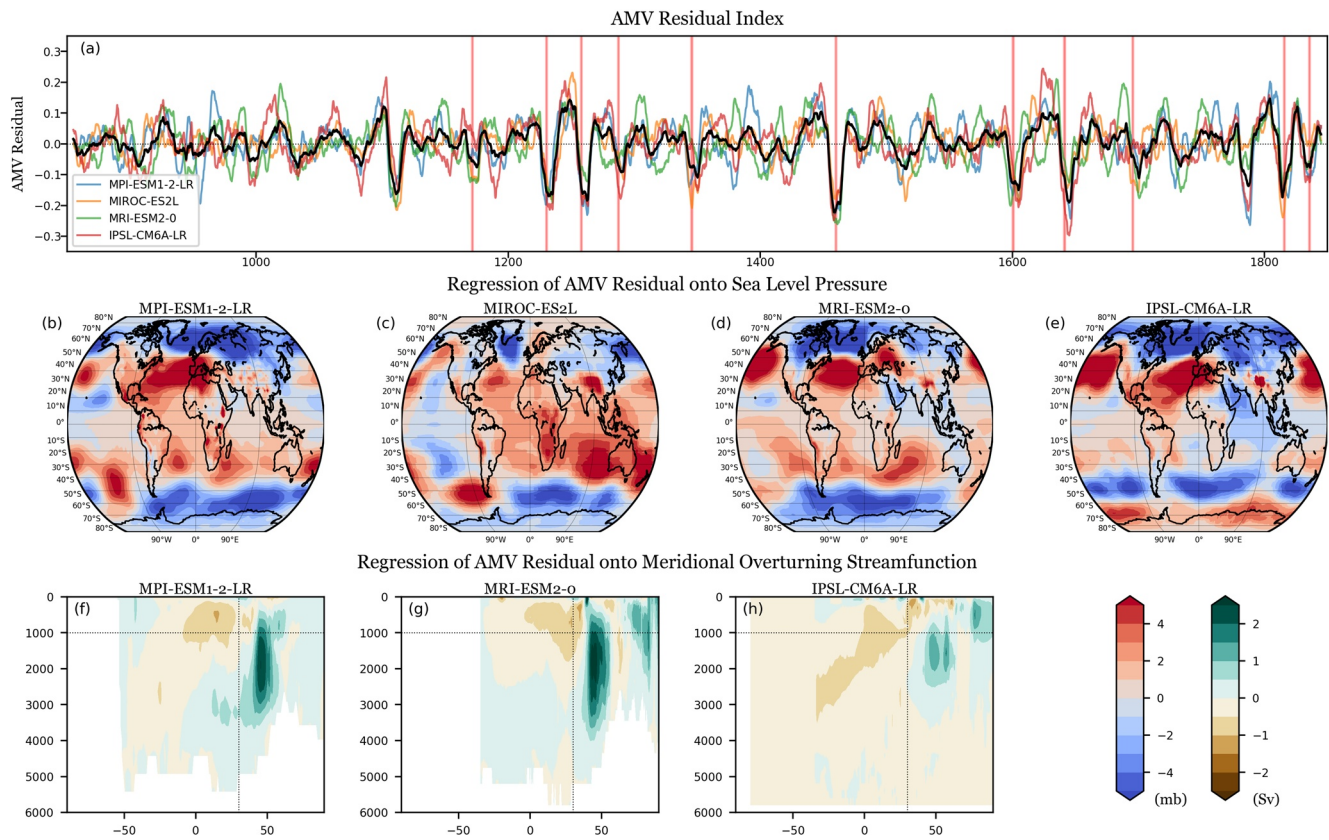


Figure 3. As in Figure 2, but for the AMV-Residual index.

over the northern hemisphere (Figure S5). That is, the spatial-average SST over the North Atlantic Ocean (i.e., the typical-AMV) includes a global cooling signature from strong tropical volcanic eruptions (and other forcing), whose basin-wide temperature change weakens the tripole structure observed from the internal component of AMV (i.e., pattern-AMV in past1000 or typical-AMV in piControl).

The regression of the meridional overturning streamfunction (Figures 3f–3h) shows that the AMV-residual has limited signature of AMOC in its tropical branch, where the streamfunction climatology has its maximum; whereas the larger response concentrates consistently over models in the mid-latitude and subpolar branch with a weaker strength compared to the pattern-AMV. The negative values of the AMV-residual after volcanic eruptions, therefore, manifest a reduction of meridional streamfunction in the mid-latitude and subpolar branch of AMOC. This is consistent with Zanchettin et al. (2012) who found that weakening of meridional streamfunction happens in the mid-latitude and subpolar branch of AMOC right after (<5 years) strong tropical volcanic eruptions. The result is not contradictory to the general finding of enhanced AMOC after volcanic eruption (Ding et al., 2014). This is because the regression represents instantaneous responses to volcanic eruptions, while the enhanced AMOC reported in the literature refers to the state 10 years after volcanic eruptions with different timing for individual models. In fact, the AMOC calculated from its tropical branch is insignificantly enhanced around 10–20 years after volcanic eruptions depending on model characteristics, shown in composite analysis (Figure S6).

To further study the relations between AMV and AMOC over the past millennium, we calculate the cross-correlations between the AMOC index and multiple AMV indices (Figures 4a–4c). The cross-correlation profiles between typical-AMV and AMOC vary substantially across models concerning magnitude and timing of the peak: correlation is strong for MPI-ESM1-2-LR and MRI-ESM2-0 but weak in IPSL-CM6A-LR; the peak value occurs when AMOC leads by about one year in MPI-ESM1-2-LR and by about 5 years in MRI-ESM2-0, while when it lags by about 1 year in IPSL-CM6A-LR. These differences may be related to the strength of AMOC variability (Yan et al., 2018), where weaker AMOC has a weaker relation with AMV as in IPSL-CM6A-LR. The

Relations between AMVs and AMOC

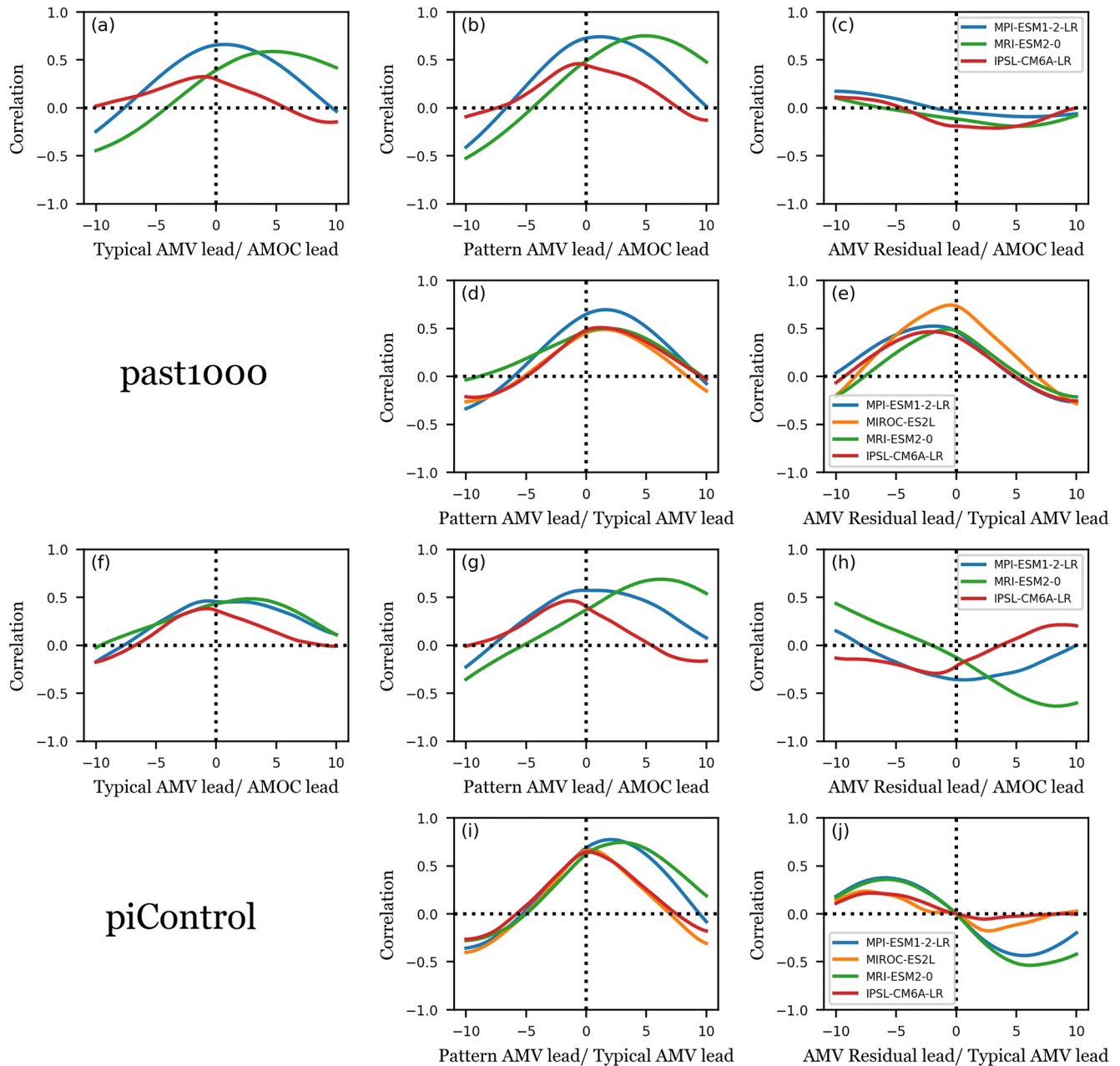


Figure 4. (a) Cross-correlations (x -axis: year unit) between AMOC and typical-AMV of past1000; (b) for pattern-AMV; (c) for AMV-residual; (d) between typical-AMV and pattern-AMV; (e) between typical-AMV and AMV-residual. (e)–(j) are for piControl.

pattern-AMV shows stronger correlations with AMOC and the AMV-residual has smaller correlations (<0.25) with AMOC than the typical-AMV for all models. The lead-lag correlation profile for typical-AMV and pattern-AMV are similar; whereas the AMV-residual is distinct. In terms of explained variance, internal variability thus dominates the relation of AMV with AMOC with unique characteristics for each model.

Furthermore, the cross-correlation profile of each model expresses a similar shape between the past1000 and piControl simulations (Figures 4f–4h), especially for the pattern-AMV. This confirms that the proposed pattern-based separation of the AMV efficiently extracting the internal AMV, and that the AMOC is predominantly linked with internal AMV. Compared to the pattern- and typical-AMV (Figures 4f and 4g), the AMV-residual in

the piControl run (Figure 4h) has an opposite relation with the AMOC. As no varying external forcing is imposed in piControl, the AMV-residual can be simply considered as an artifact that compensates for the internal variability of AMV. This entails the internal component of AMV is difficult to be represented with one single climate mode/index, or the North Atlantic uniform SST changes may be impacted by the fluctuations of internal AMV.

To understand the relation between the three AMV indices, Figures 4d, 4e, 4i and 4j show the cross-correlation between the three AMV indices. In the past1000 simulation, the pattern-AMV and the AMV-residual both have positive correlations with the typical-AMV, indicating both the internal and external signature combine to explain the North Atlantic variability. For the residual-typical AMV relation, the largest correlation exists when the AMV-residual leads the typical-AMV by 2–3 years. This reveals the external forcing such as volcanic eruption can impact the AMV and imprint the signature for a few years. On the other hand, the largest correlation between the typical-AMV and the pattern-AMV exists when the typical-AMV leads the pattern-AMV by 2–3 years. This reveals that, besides the tripole structure, other SST changes in the North Atlantic Ocean may continue to warm/cool the region for a few years with a manifestation of the tripole structure; However, more detailed analyses are needed in the future.

The relations between AMV indices also changes from the piControl simulations to the past1000 simulations. The peak correlation between the pattern-AMV and the typical-AMV drops by about 0.1 from the piControl to the past1000 run, indicating that the external forcing contributes to the AMV and reduces the relative importance of the internal AMV component, but does so only marginally. In piControl, the AMV-residual is uncorrelated with the typical-AMV index at lag 0, but the correlation is around 0.5 in past1000. So, external forcing can explain about 25% of the AMV in the past1000, which implies that the internal component of the AMV still dominates the total variability. We noticed that there is a possibility for the AMV-residual to impact the internal variability, which will need to be further investigated in the future.

4. Summary and Discussion

This study demonstrates that the classical AMV, or typical-AMV, can be separated into the internal AMV and the external signal by a spatial pattern regression method, where the former component is captured by the pattern-AMV index and the latter by the AMV-residual index. Over the past millennium, the pattern-AMV shows a tripole SST structure and the index has limited response to volcanic eruptions. A strong relation between the pattern-AMV and the meridional overturning circulation or AMOC is found. On the other hand, the AMV-residual shows an SST structure that represents global temperature changes, particularly those related to strong tropical volcanic eruptions. The radiative cooling after strong eruptions imprints onto the AMV-residual index with an initial negative phase typically followed by a warm phase (or neutral) after 5 years, yielding an apparent oscillatory response. This surface forcing from the AMV-residual has a consistent reduction of AMOC of its mid-latitude and subpolar branch across models, but weak enhancement is found in AMOC index related to its tropical branch after eruptions. This reveals the natural external forcing over pre-industrial millennium may have less impacts than the anthropogenic forcing in recent decades (Caesar et al., 2018; Chemke et al., 2020). The strong relation between the pattern-AMV and AMOC indicates a domination of internal variability of AMOC and limited impacts on AMOC from external forcing.

Furthermore, as previous studies have shown that volcanic forcing can imprint onto North Atlantic Ocean (Otterå et al., 2010; Zanchettin et al., 2012), this study extends the discussion by providing an explanation of why the tripole structure of AMV cannot be found in some AMV calculations and assessing the relative contribution from the internal and external forcing. The internal component of AMV in past1000 has a tripole SST structure as in piControl, while the external component shows a global temperature change. This entails that the AMV without the tripole structure may include the signature from the external forcing (Otterå et al., 2010; Zhang et al., 2019). We found that the external forcing explains ~25% of the AMV variation in transient conditions. That is, the internal AMV component dominates the strength and variation of AMV over the past millennium and the external forcing fluctuates the AMV but not having direct impacts in the long term (Figure S7). Since the past1000 simulations only include volcanic stratospheric aerosol but not anthropogenic aerosol, the relative importance of external forcing may be different for recent decades (Booth et al., 2012; Qin et al., 2020b).

Comparing the unforced (piControl) and forced (past1000) simulations from CMIP5, Mann et al. (2021) found that the internal AMV has no specific time-scale across models whereas volcanic eruptions can project onto the

multi-decadal (50–70 years) period. In this study, we show that the typical spatial pattern reflecting AMV in piControl simulations (the internal or pattern AMV) is robust across models, but each model has its own characteristic AMV-AMOC relation (Figure 4g), where the time-scale may not be matched. For example, the peak value of cross correlation between AMV and AMOC occurs when AMOC leads by about one and five years in MPI-ESM1-2-LR and MRI-ESM2-0, whereas it lags by about one year in IPSL-CM6A-LR. Also, the external forcing (especially the volcanic eruptions) cannot disrupt/change the existing AMV-AMOC relation that has been observed in the unperturbed run, indicating the dominance of the internal AMV in controlling the AMV.

Data Availability Statement

The Python codes for generating the figures and the processed data of the variables from piControl and past1000 simulations can be accessed at Zenodo with DOI: <https://zenodo.org/record/5256891#.YYmIFU7MKUI>.

Acknowledgments

We thank two anonymous reviewers for their valuable comments and Jürgen Bader who gave valuable comments on an earlier version of this paper. The research for SWF is funded by the German Federal Ministry of Education and Research (BMBF), research programme “ROMIC-II, ISOVIC” (FKZ: 01LG1909 B). CT acknowledges support to this research by the Deutsche Forschungsgemeinschaft Research Unit VolImpact (FOR2820, grant no. 398006378) within the project VolClim (TI 344/2-1). MK acknowledges support from L-IPSL LABEX, the IPSL Climate Graduate School EUR, CALDERA project grant and the HPC resources of TGCC under the allocations 2020-A0080107732 and 2021-A0100107732 (project genemip6) provided by GENCI (Grand Equipment National de Calcul Intensif) and 2020225424 provided by PRACE. The computations, analysis and model data storage were mainly performed on the computer of the Deutsches Klima Rechenzentrum (DKRZ) using resources granted by its Scientific Steering Committee (WLA) under project ID bb1171. We acknowledge the World Climate Research Programme's Working Group on Coupled Modeling, which is responsible for PMIP, and we thank the climate modeling groups (listed in Extended Data Table S1) for producing and making available their model output (Boucher et al., 2018; Hajima et al., 2019; Ohgaito et al., 2020; Wieners et al., 2019; Yukimoto et al., 2019b, 2020). The analyses were performed using Python. Open access funding enabled and organized by Projekt DEAL.

References

- Booth, B. B., Dunstone, N. J., Halloran, P. R., Andrews, T., & Bellouin, N. (2012). Aerosols implicated as a prime driver of twentieth-century North Atlantic climate variability. *Nature*, *484*(7393), 228–232.
- Boucher, O., Denvil, S., Levavasseur, G., Cozic, A., Caubel, A., FoujolsMarie-Alice, et al. (2018). *IPSL IPSL-CM6A-LR model output prepared for CMIP6 CMIP esm-piControl*. Earth System Grid Federation.
- Boucher, O., Servonnat, J., Albright, A. L., Aumont, O., Balkanski, Y., Bastrikov, V., & Vuichard, N. (2020). Presentation and evaluation of the IPSL-CM6A-LR climate model. *Journal of Advances in Modeling Earth Systems*, *12*(7), e2019MS002010.
- Caesar, L., Rahmstorf, S., Robinson, A., Feulner, G., & Saba, V. (2018). Observed fingerprint of a weakening Atlantic Ocean overturning circulation. *Nature*, *556*(7700), 191–196.
- Chemke, R., Zanna, L., & Polvani, L. M. (2020). Identifying a human signal in the North Atlantic warming hole. *Nature Communications*, *11*(1), 1–7.
- Chiang, J. C., & Vimont, D. J. (2004). Analogous Pacific and Atlantic meridional modes of tropical atmosphere–ocean variability. *Journal of Climate*, *17*(21), 4143–4158.
- Clement, A., Bellomo, K., Murphy, L. N., Cane, M. A., Mauritsen, T., Rädel, G., & Stevens, B. (2015). The Atlantic multidecadal oscillation without a role for ocean circulation. *Science*, *350*(6258), 320–324.
- Czaja, A., & Frankignoul, C. (2002). Observed impact of Atlantic SST anomalies on the North Atlantic Oscillation. *Journal of Climate*, *15*(6), 606–623.
- Ding, Y., Carton, J. A., Chepurin, G. A., Stenchikov, G., Robock, A., Sentman, L. T., & Krasting, J. P. (2014). Ocean response to volcanic eruptions in Coupled Model Intercomparison Project 5 (CMIP5) simulations. *Journal of Geophysical Research: Ocean*, *119*, 5622–5637. <https://doi.org/10.1002/2013JC009780>
- Dong, B., Sutton, R. T., & Scaife, A. A. (2006). Multidecadal modulation of El Niño–Southern Oscillation (ENSO) variance by Atlantic Ocean sea surface temperatures. *Geophysical Research Letters*, *33*(8).
- Enfield, D. B., Mestas-Núñez, A. M., & Trimble, P. J. (2001). The Atlantic multidecadal oscillation and its relation to rainfall and river flows in the continental US. *Geophysical Research Letters*, *28*(10), 2077–2080.
- Friedman, A. R., Reverdin, G., Khodri, M., & Gastineau, G. (2017). A new record of Atlantic sea surface salinity from 1896 to 2013 reveals the signatures of climate variability and long-term trends. *Geophysical Research Letters*, *44*(4), 1866–1876.
- Goldenberg, S. B., Landsea, C. W., Mestas-Núñez, A. M., & Gray, W. M. (2001). The recent increase in Atlantic hurricane activity: Causes and implications. *Science*, *293*(5529), 474–479.
- Hajima, T., Abe, M., Arakawa, O., Suzuki, T., Komuro, Y., Ogura, T., et al. (2019). *MIROC MIROC-ES2L model output prepared for CMIP6 CMIP piControlEarth System Grid Federation*. Version 20190823. <https://doi.org/10.22033/ESGF/CMIP6.5710>
- Jungclauss, J. H., Bard, E., Baroni, M., Braconnot, P., Cao, J., Chini, L. P., & Zorita, E. (2017). The PMIP4 contribution to CMIP6–Part 3: The last millennium, scientific objective, and experimental design for the PMIP4 past1000 simulations. *Geoscientific Model Development*, *10*(11), 4005–4033.
- Kageyama, M., Braconnot, P., Harrison, S. P., Haywood, A. M., Jungclauss, J. H., Otto-Bliesner, B. L., & Zhou, T. (2018). The PMIP4 contribution to CMIP6–Part 1: Overview and over-arching analysis plan. *Geoscientific Model Development*, *11*(3), 1033–1057.
- Knight, J. R., Folland, C. K., & Scaife, A. A. (2006). Climate impacts of the Atlantic multidecadal oscillation. *Geophysical Research Letters*, *33*(17).
- Li, X., Holland, D. M., Gerber, E. P., & Yoo, C. (2014). Impacts of the north and tropical Atlantic Ocean on the Antarctic Peninsula and sea ice. *Nature*, *505*(7484), 538–542.
- Lurton, T., Balkanski, Y., Bastrikov, V., Bekki, S., Bopp, L., Braconnot, P., & Boucher, O. (2020). Implementation of the CMIP6 forcing data in the IPSL-CM6A-LR model. *Journal of Advances in Modeling Earth Systems*, *12*(4), e2019MS001940.
- Mann, M. E., Steinman, B. A., Brouillette, D. J., & Miller, S. K. (2021). Multidecadal climate oscillations during the past millennium driven by volcanic forcing. *Science*, *371*(6533), 1014–1019.
- Martin, E. R., Thorncroft, C. D., & Booth, B. B. B. (2014). The multidecadal Atlantic SST–Sahel rainfall teleconnection in CMIP5 simulations. *Journal of Climate*, *27*, 784–806. <https://doi.org/10.1175/JCLI-D-13-00242.1>
- Mauritsen, T., Bader, J., Becker, T., Behrens, J., Bittner, M., Brokopf, R., & Roeckner, E. (2019). Developments in the MPI-M Earth System Model version 1.2 (MPI-ESM1.2) and its response to increasing CO₂. *Journal of Advances in Modeling Earth Systems*, *11*(4), 998–1038.
- Oelsmann, J., Borchert, L., Hand, R., Baehr, J., & Jungclauss, J. H. (2020). Linking Ocean Forcing and Atmospheric Interactions to Atlantic multidecadal variability in MPI-ESM1.2. *Geophysical Research Letters*, *47*(10), e2020GL087259.
- Ohgaito, R., Abe-Ouchi, A., Abe, M., Arakawa, O., Ogochi, K., Hajima, T., et al. (2020). *MIROC MIROC-ES2L model output prepared for CMIP6 PMIP past1000*. Version 20200318. Earth System Grid Federation. <https://doi.org/10.22033/ESGF/CMIP6.5666>
- Ohgaito, R., Yamamoto, A., Hajima, T., Oishi, R., Abe, M., Tatebe, H., & Kawamiya, M. (2021). PMIP4 experiments using MIROC-ES2L Earth system model. *Geoscientific Model Development*, *14*(2), 1195–1217.

- O'Reilly, C. H., Woollings, T., & Zanna, L. (2017). The dynamical influence of the Atlantic multidecadal oscillation on continental climate. *Journal of Climate*, *30*(18), 7213–7230.
- O'Reilly, C. H., Zanna, L., & Woollings, T. (2019). Assessing external and internal sources of Atlantic multidecadal variability using models, proxy data, and early instrumental indices. *Journal of Climate*, *32*(22), 7727–7745.
- Otterå, O. H., Bentsen, M., Drange, H., & Suo, L. (2010). External forcing as a metronome for Atlantic multidecadal variability. *Nature Geoscience*, *3*(10), 688–694.
- Qin, M., Dai, A., & Hua, W. (2020a). Quantifying contributions of internal variability and external forcing to Atlantic multidecadal variability since 1870. *Geophysical Research Letters*, *47*(22), e2020GL089504.
- Qin, M., Dai, A., & Hua, W. (2020b). Aerosol-forced multidecadal variations across all ocean basins in models and observations since 1920. *Science Advances*, *6*(29), eabb0425.
- Ruprich-Robert, Y., Delworth, T., Msadek, R., Castruccio, F., Yeager, S., & Danabasoglu, G. (2018). Impacts of the Atlantic multidecadal variability on North American summer climate and heat waves. *Journal of Climate*, *31*(9), 3679–3700.
- Ruprich-Robert, Y., Moreno-Chamarro, E., Levine, X., Bellucci, A., Cassou, C., Castruccio, F., & Tourigny, E. (2021). Impacts of Atlantic multidecadal variability on the tropical Pacific: A multi-model study. *NPJ Climate and Atmospheric Science*, *4*(1), 1–11.
- Sutton, R. T., & Dong, B. (2012). Atlantic Ocean influence on a shift in European climate in the 1990s. *Nature Geoscience*, *5*(11), 788–792.
- Sutton, R. T., & Hodson, D. L. (2005). Atlantic Ocean forcing of North American and European summer climate. *Science*, *309*(5731), 115–118.
- Villamayor, J., Mohino, E., Khodri, M., Mignot, J., & Janicot, S. (2018). Atlantic control of the late nineteenth-century Sahel humid period. *Journal of Climate*, *31*(20), 8225–8240.
- Wallace, J. M., Smith, C., & Jiang, Q. (1990). Spatial patterns of atmosphere-ocean interaction in the northern winter. *Journal of Climate*, *3*(9), 990–998.
- Wang, J., Yang, B., Ljungqvist, F. C., Luterbacher, J., Osborn, T. J., Briffa, K. R., & Zorita, E. (2017). Internal and external forcing of multidecadal Atlantic climate variability over the past 1,200 years. *Nature Geoscience*, *10*(7), 512–517.
- Wieners, K.-H., Giorgetta, M., Jungclaus, J., Reick, C., Esch, M., Bittner, M., et al. (2019). *MPI-M MPI-ESM1.2-LR model output prepared for CMIP6 CMIP esm-piControl*. Version 20190710. Earth System Grid Federation. <https://doi.org/10.22033/ESGF/CMIP6.6553>
- Wu, B., Lin, X., & Yu, L. (2020). North Pacific subtropical mode water is controlled by the Atlantic multidecadal variability. *Nature Climate Change*, *10*(3), 238–243.
- Yan, X., Zhang, R., & Knutson, T. R. (2018). Underestimated AMOC variability and implications for AMV and predictability in CMIP models. *Geophysical Research Letters*, *45*(9), 4319–4328.
- Yan, X., Zhang, R., & Knutson, T. R. (2019). A multivariate AMV index and associated discrepancies between observed and CMIP5 externally forced AMV. *Geophysical Research Letters*, *46*(8), 4421–4431.
- Yu, J. Y., Kao, P. K., Paek, H., Hsu, H. H., Hung, C. W., Lu, M. M., & An, S. I. (2015). Linking emergence of the central Pacific El Niño to the Atlantic multidecadal oscillation. *Journal of Climate*, *28*(2), 651–662.
- Yukimoto, S., Kawai, H., Koshiro, T., Oshima, N., Yoshida, K., Urakawa, S., & Ishii, M. (2019). The Meteorological Research Institute Earth System Model version 2.0, MRI-ESM2.0: Description and basic evaluation of the physical component. *Journal of the Meteorological Society of Japan. Ser. II*.
- Yukimoto, S., Koshiro, T., Kawai, H., Oshima, N., Yoshida, K., Urakawa, S., et al. (2019). *MRI MRI-ESM2.0 model output prepared for CMIP6 CMIP piControlEarth System Grid Federation*. Version 20190904. <https://doi.org/10.22033/ESGF/CMIP6.6900>
- Yukimoto, S., Koshiro, T., Kawai, H., Oshima, N., Yoshida, K., Urakawa, S., et al. (2020). *MRI MRI-ESM2.0 model output prepared for CMIP6 PMIP past1000*. Version 20200303. Earth System Grid Federation. <https://doi.org/10.22033/ESGF/CMIP6.6866>
- Zanchettin, D., Bothe, O., Graf, H. F., Omrani, N. E., Rubino, A., & Jungclaus, J. H. (2016). A decadal delayed response of the tropical Pacific to Atlantic multidecadal variability. *Geophysical Research Letters*, *43*(2), 784–792.
- Zanchettin, D., Bothe, O., Müller, W., Bader, J., & Jungclaus, J. H. (2014). Different flavors of the Atlantic multidecadal variability. *Climate Dynamics*, *42*(1), 381–399.
- Zanchettin, D., Bothe, O., Rubino, A., & Jungclaus, J. H. (2016). Multi-model ensemble analysis of Pacific and Atlantic SST variability in unperturbed climate simulations. *Climate Dynamics*, *47*(3), 1073–1090.
- Zanchettin, D., Rubino, A., Matei, D., Bothe, O., & Jungclaus, J. H. (2013). Multidecadal-to-centennial SST variability in the MPI-ESM simulation ensemble for the last millennium. *Climate Dynamics*, *40*(5–6), 1301–1318.
- Zanchettin, D., Timmreck, C., Graf, H.-F., Rubino, A., Lorenz, S., Lohmann, K., et al. (2012). Bi-decadal variability excited in the coupled ocean-atmosphere system by strong tropical volcanic eruptions. *Climate Dynamics*, *39*(1), 419–444.
- Zhang, R., & Delworth, T. L. (2006). Impact of Atlantic multidecadal oscillations on India/Sahel rainfall and Atlantic hurricanes. *Geophysical Research Letters*, *33*(17).
- Zhang, R., Sutton, R., Danabasoglu, G., Delworth, T. L., Kim, W. M., Robson, J., & Yeager, S. G. (2016). Comment on “The Atlantic Multidecadal Oscillation without a role for ocean circulation”. *Science*, *352*(6293), 1527–1527.
- Zhang, R., Sutton, R., Danabasoglu, G., Kwon, Y. O., Marsh, R., Yeager, S. G., & Little, C. M. (2019). A review of the role of the Atlantic meridional overturning circulation in Atlantic multidecadal variability and associated climate impacts. *Reviews of Geophysics*, *57*(2), 316–375.